Two New Super Li-rich Core He-burning Giants: A New Twist to the Long Tale of Li Enhancement in K Giants

Yerra Bharat Kumar[1] , Raghubar Singh[2], B. Eswar Reddy[2], and Gang Zhao[1,3]

[1] Key Laboratory of Optical Astronomy, National Astronomical Observatories, Chinese Academy of Sciences,
Beijing 100012, People's Republic of China; bharat@bao.ac.cn
[2] Indian Institute of Astrophysics, Koramangala II Block, Bangalore 560034, India
[3] School of Astronomy and Space Science, University of Chinese Academy of Sciences, Beijing 100049, People's Republic of China

Abstract

In this Letter we report two new super Li-rich K giants, KIC2305930 and KIC12645107, with Li abundances exceeding that of the interstellar medium (ISM; $A(Li) \geqslant 3.2$ dex). Importantly, both of the giants have been classified as core He-burning red clump (RC) stars based on asteroseismic data from *Kepler* mission. Also, both of the stars are found to be low mass ($M \approx 1.0 \, M_\odot$), which, together with an evidence of their evolutionary status of being RC stars, implies that the stars have gone through both the luminosity bump and He-flash during their red giant branch (RGB) evolution. The stars' large Li abundance and evolutionary phase suggest that Li enrichment occurred very recently, probably at the tip of the RGB either during He-flash, an immediate preceding event on the RGB, or by some kind of external event such as merger of an RGB star with white dwarf. The findings will provide critical constraints to theoretical models for understanding of Li enhancement origin in RGB stars.

Key words: stars: abundances – stars: evolution – stars: individual (KIC2305930, KIC12645107) – stars: late-type – stars: low-mass

1. Introduction

Contrary to theoretical expectations, a small class of red giant branch (RGB) stars show an overabundance of Li in their photosphere. The expectation is that Li will be severely depleted as a result of the first dredge-up and deep convective envelope in low-mass stars from its initial value of main sequence, and should not exceed $A(Li) = 1.5$ dex in RGB stars (e.g., Iben 1967). In fact, observations show much less Li abundance (Brown et al. 1989) than the expected maximum value in RGB stars. This may be due in part to some Li depletion during main sequence and pre-main sequence phases. For example, the Sun has Li abundance of $A(Li) \sim 1.0$ dex, which is about two orders of magnitude less than the initial Population I main-sequence value of $A(Li) \sim 3.3$ dex (e.g., Lambert & Reddy 2004). Thus, finding large Li abundances in RGB stars and, in some cases, exceeding that of the interstellar medium (ISM) value, is puzzling.
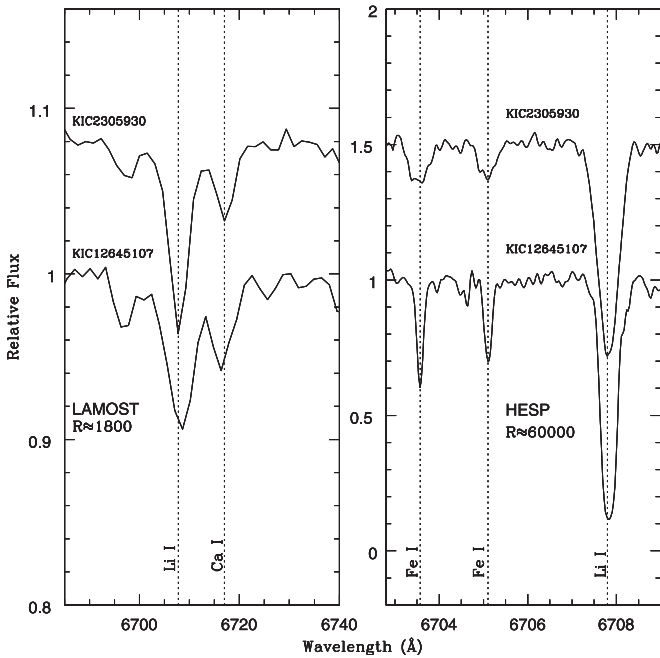
Studies from systematic surveys found that Li-rich RGB stars are rare, making up just about 1% of all RGB stars, irrespective of stellar populations (Brown et al. 1989; Kumar et al. 2011; Monaco et al. 2011; Li et al. 2018). Now there are more than 100 ($\sim$150) Li-rich stars, of which a dozen are super-Li rich stars with $A(Li) \geqslant 3.2$ dex (see Casey et al. 2016 and references therein). The rarity of Li-rich stars indicate that Li enrichment on the RGB is a transient phenomenon. However, it is not understood how or at what stage of the RGB phase such Li enrichment occurs. This has been a question to be answered ever since the first Li-rich K giant was discovered by Wallerstein & Sneden (1982).

One of the obstacles hindering the understanding of the Li origin in K giants has been the lack of data from which their location in the Hertzsprung–Russel (HR) diagram can be fixed unambiguously. This is mainly due to uncertainties in derived key parameters: luminosity and $T_{\rm eff}$ which, in most cases, exceed the difference in $T_{\rm eff}$-luminosity space between the

suggested locations of Li-enrichment on the RGB. For example, distinguishing stars of the red clump (RC) region post He-flash from the luminosity bump region is difficult. In particular, consider the case of Population I stars in which the two regions in the HR diagram are separated just by 50–300 K in $T_{\rm eff}$, and 0.1–0.4 dex in luminosity, depending on metallicity and mass (Girardi 2016). As a result, studies solely based on spectroscopy and photometry cannot draw conclusions on the origin of Li enhancement. Though astrometry from space-based *Hipparcos* or *Gaia* missions provides relatively precise luminosities, they cannot resolve positional uncertainty of Li-rich K giants on the RGB (Kumar & Reddy 2009; Kumar et al. 2011). This may be the reason why many observational results show Li-rich K giants in overlapping regions in the HR diagram: below the luminosity bump (Martell & Shetrone 2013; Casey et al. 2016; Li et al. 2018), at the bump (Charbonnel & Balachandran 2000; Kumar & Reddy 2009), well above the bump closer to the RGB tip (Monaco et al. 2011), and the RC (Kumar et al. 2011; Silva Aguirre et al. 2014).

The lack of clarity regarding the precise location of Li-rich giants on the RGB has led to interesting speculations and theoretical modeling. These range from external causes, such as the engulfment of material of unburnt Li in massive planets (Siess & Livio 1999; Denissenkov & Herwig 2004) and the accretion of material enriched with Li due to spallation in binary companion supernova explosions or strong outbursts in X-ray binary systems (e.g., Tajitsu et al. 2015), to in situ synthesis and the dredge-up of Li-rich material to the photosphere.

The current impasse may be addressed using asteroseismology, which is regarded as a standard tool to separate stars of the core-He-burning RC phase from the inert He-core hydrogen-shell-burning RGB phase. The *Kepler* space mission provides high-precision photometry capable of measuring frequencies sensitive to stellar evolutionary phases. Here, we report two new *Kepler* field super Li-rich stars based on the Large Sky Area Multi-Object

Figure 1. Li resonance line at 6707 Å in the LAMOST and HESP spectra of two sample stars.

Table 1
Derived Results of New Super Li-rich RC Giants

Parameters	KIC2305930	KIC12645107
$T_{\rm eff}$(Spec)	4750 ± 80	4850 ± 50
$T_{\rm eff}$(Phot)	4800 ± 90	4765 ± 90
$T_{\rm eff}$(LAMOST)	4875 ± 86	4841 ± 80
$T_{\rm eff}$(APOGEE)	4750 ± 70	4825 ± 70
$\log g_{\rm Spec}$	2.38 ± 0.1	2.62 ± 0.1
$\log g_{\rm Seism}$	2.37 ± 0.01	2.37 ± 0.01
$\log(L/L_{\odot})$[b]	2.0	1.75
$M/M_{\odot}$	0.92 ± 0.11	1.05 ± 0.04
$v\sin i$	12.5 ± 1	1.5 ± 0.5
$[Fe/H]$	-0.5 ± 0.1	-0.2 ± 0.05
A(Li)LTE	4.2	3.24
A(Li)NLTE	3.88	3.38
[C/Fe]	0.36[a]	-0.40
[N/Fe]	0.10[a]	0.54
[C/N]	0.27	-0.94
^{12}C/^{13}C	10 ± 2	6 ± 1

Note.
[a] APOGEE DR13.
[b] From GAIA DR1 Parallaxes.

Fiber Spectroscopic Telescope (LAMOST) survey and subsequent high-resolution spectra. The findings in this Letter will help to constrain theoretical aspects of Li enrichment in RGB stars.

2. Sample Selection and Observations

LAMOST, a reflecting Schmidt telescope containing 4000 fibers on its focal plane, observed millions of low-resolution ($R \approx 1800$) stellar spectra (Zhao et al. 2006, 2012). Based on the technique used in Kumar et al. (2018), a number of Li-rich stars have been identified among high-quality LAMOST spectra, of which two stars, J191712.49+514511.3 (KIC12645107) and J192825.63+374123.3 (KIC2305930), are found to have exceptionally strong Li line at 6707 Å. Both stars have been classified as RC stars with a He-burning core based on *Kepler* asteroseismic data.

The two super Li-rich candidates are subjected to high-resolution ($R \approx 60000$) observations using the Hanle Echelle Spectrograph (HESP) equipped to 2 m Himalayan *Chandra* Telescope (HCT) at Hanle. HESP provides spectral coverage starting from 3800 Å to 9300 Å in 56 Echelle orders without inter-order wavelength gaps. As stars are relatively fainter ($V > 11$), we obtained three spectra of 40 minutes of exposure each for KIC2305930, and two spectra of 40 minutes of exposure each for KIC12645107. For spectral calibration and removal of telluric lines we obtained spectra of a Th-Ar arc lamp and a hot star (HD149630) with rapid rotation ($v \sin i \sim 294 \,{\rm km\,s^{-1}}$), respectively. The raw two-dimensional images are reduced in standard procedure using Image Reduction and Spectral Facility (IRAF). The spectra have signal-to-noise ratio (S/N) of 50 at 6500 Å and is about 100 at 8000 Å. Spectra are wavelength calibrated and continuum fitted. Sample spectra of two stars near the Li resonance line at 6707 Å are shown in Figure 1.

3. Analysis and Results

3.1. Atmospheric Parameters and Abundances

The atmospheric parameters ($T_{\rm eff}$, $\log g$, [Fe/H], ξ_t) have been obtained using standard procedures based on high-resolution spectra and local thermodynamic equilibrium (LTE) stellar model atmospheres with convection-on (Castelli & Kurucz 2004) using an iterative process (see Kumar et al. 2011). We used an updated version of spectral analysis code *MOOG* (Sneden 1973) for deriving abundances and generating synthetic spectra. To derive accurate atmospheric parameters, a list of well-calibrated Fe I and Fe II lines was adopted from the compilation of Reddy et al. (2003) and Ramírez & Allende Prieto (2011). Equivalent widths (EWs) were measured from the radial velocity corrected spectra. The final representative atmospheric model is the one for which the abundances of element Fe are independent of the lines' low excitation potential (LEP), equivalent widths, and ionization state (in this case abundances of Fe I and Fe II lines should be same). We found best-fit models of $T_{\rm eff} = 4750 \pm 80$ K, $\log g = 2.38 \pm 0.1$ dex, [M/H] $= -0.50 \pm 0.1$ dex and $\xi_t = 1.5 \pm 0.1 \,{\rm km\,s^{-1}}$ for KIC2305930 and $T_{\rm eff} = 4850 \pm 50$ K, $\log g = 2.62 \pm 0.1$, [M/H] $= -0.20 \pm 0.05$ and $\xi_t = 1.4 \pm 0.1 \,{\rm km\,s^{-1}}$ for KIC12645107. Uncertainties in the parameters have been determined using a range of model parameters and their sensitivity to abundance trends with LEP or EWs and differences between neutral and singly ionized Fe. The derived parameters in this study are in good agreement, within uncertainties, with the values derived from APOGEE spectra (DR13: Albareti et al. 2017, see Table 1). The derived values of $T_{\rm eff}$ based on 2MASS photometry and calibrations of González Hernández & Bonifacio (2009) are in very good agreement with the spectroscopic values. However, $\log g$ value derived using asteroseismic data (Pinsonneault et al. 2014; Vrard et al. 2016) for KIC12645107 are found to be about 0.25 dex more than the spectroscopic value. Derived
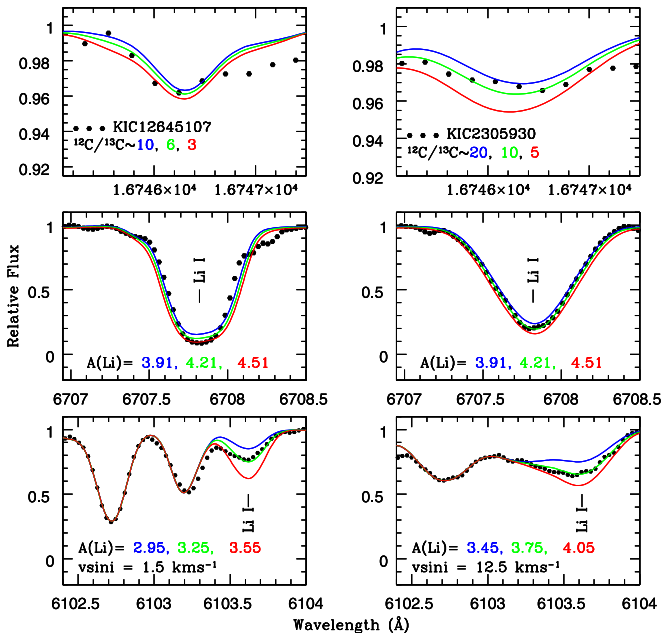
Figure 2. Derivation of $^{12}C/^{13}C$ ratios (top two panels) and Li abundances from Li resonance line and subordinate lines (bottom four panels) for two stars.

Figure 3. Location of the two sample stars on HR diagram (left) and seismic diagram (right). Blue symbols are from Vrard et al. (2016). Note that both stars occupy the core He-burning region in both panels.

atmospheric and other stellar parameters, along with literature values, are given in Table 1. Spectroscopic values are adopted for further analysis.

Abundance of Li has been derived using Li resonance line 6707.8 Å and the subordinate line 6103.6 Å. We adopted spectral synthesis using LTE model atmospheres as described in Kumar et al. (2011) for deriving Li abundance. Atomic data including line list and *gf*-values are taken from the compilation of Reddy et al. (2002). Hyperfine features are taken from Hobbs et al. (1999). Final abundances are corrected for non-LTE using a recipe given by Lind et al. (2009).[4] The spectral synthesis of Li lines at 6707 Å and 6103 Å are shown in Figure 2. The derived Li abundances based on high resolution confirm that the stars are super Li-rich K giants as identified from the LAMOST low-resolution spectra.

Further, we derived C and N abundances and carbon isotopic ratio ($^{12}C/^{13}C$), which are key diagnostics for the stars' evolutionary phase and level of mixing. Carbon abundance is derived from C I lines at 5052 Å and 5380 Å. However, the N abundance is based on molecular lines $^{12}C^{14}N$ by matching the observed spectrum with the synthetic spectrum in the region of 8003 Å to 8012 Å. Line list and molecular data such as dissociation energies and *gf*-values are taken from Sneden et al. (2014). However, C and N lines in the spectra of KIC2305930 are smeared out due to relatively high stellar rotation and are too weak for abundance determination. As a result, we adopted [C/Fe] and [N/Fe] from the APOGEE DR13 catalog based on infrared spectra for this star. Using C and N abundances as input, we obtained $^{12}C/^{13}C$ ratios using $^{13}C^{14}N$ line at 8004.6 Å by performing spectral synthesis as described in Kumar & Reddy (2009). We also synthesized 16745.3–16746.9 Å region in H-band APOGEE spectra[5] to derive $^{12}C/^{13}C$ (See Figure 2) in a similar fashion described in
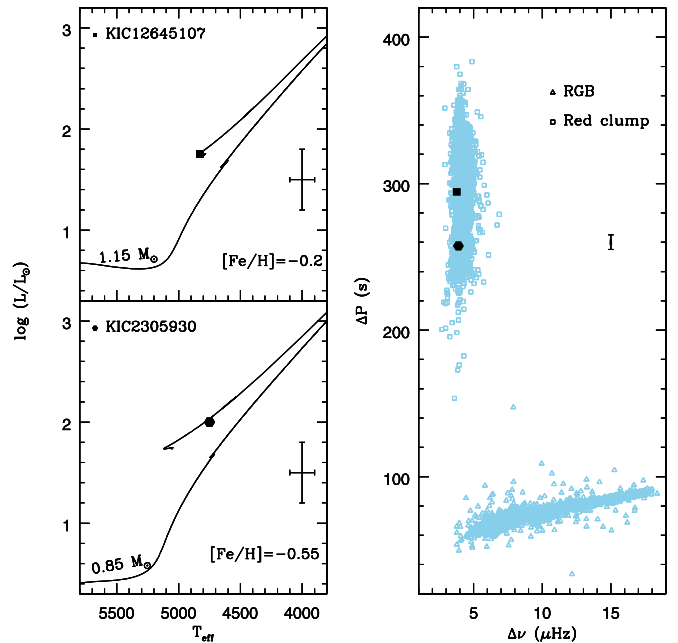
Szigeti et al. (2018). The atmospheric parameters, elemental abundances, and isotopic ratios are given in Table 1.

3.2. Mass, v sin i, and Infrared Excess

For both the stars, masses have been derived using *Kepler* asteroseismic data combined with our spectroscopic T_{eff} values using the relation given in Kjeldsen & Bedding (1995). Based on seismic values given in Vrard et al. (2016), we obtained a mass of $1.05 M_\odot$ for KIC12645107. Similarly, for KIC2305930, we obtained a mass of $0.92 M_\odot$ using seismic values given in Mosser et al. (2014). Projected rotational velocities ($v \sin i$) have been derived using two Fe I lines (See Figure 1) adjacent to the Li line as described in Reddy et al. (2002), in which macroturbulence (V_m) and $v \sin i$ are estimated simultaneously for a given Fe I abundance and instrumental profiles by using the χ^2 test. This method resulted in $v \sin i$ values of 1.5 ± 0.5 km s^{-1} and 12.5 ± 1.0 km s^{-1} for KIC12645107 and KIC2305930, respectively. Also, both stars have been searched for possible IR excess using IR photometry from 2MASS and *WISE* (Cutri et al. 2003, 2013). Comparison of observed IR fluxes with model spectral energy distribution, and the color criteria for IR excess suggested by Rebull et al. (2015) and Bharat Kumar et al. (2015) do not indicate IR excess in either of the two stars.

4. Discussion

We found two new Li-rich stars for which the RC evolutionary phase is known from an independent analysis of asteroseismic data (See Figure 3). Including these two, there are now three bonafide Li-rich core-He-burning RC stars. The other one is a Li-rich K giant, KIC5000307 (Silva Aguirre et al. 2014). It has an Li abundance of A(Li) = 2.71 dex with an estimated mass of $1.52 M_\odot$. In comparison to this, the two new stars reported here are super-Li rich (A(Li) $\geqslant$ 3.2 dex) and of solar mass ($\sim 1 M_\odot$). Also, there exists another Li-rich star, KIC9821622 (Jofré et al. 2015), which has been classified based on asteroseismology as an RGB star with an He-inert core.

---

[4]   http://inspect-stars.com/
[5]   https://dr13.sdss.org/infrared/spectrum/search

Its $T_{\rm eff}$ and luminosity places the star below the luminosity bump. The reported Li abundance for this star is in the range of 1.65–1.94 dex. However, KIC9821622 is peculiar due to its unusual α- and s-process elements, which is atypical for Li-rich RGB stars.

There are two broad scenarios for Li origin: (a) internal production that is specific to a particular location, and (b) external origin that is not specific to any particular location. Let us first look at internal production scenarios, which are associated with internal changes to stellar structure such as extra mixing at the luminosity bump or He-flash at the RGB tip. At the luminosity bump, low-mass Population I stars are expected to experience extra mixing. At the bump, giants will have a central He-core surrounded by an H-burning shell above which there is a radiative zone that inhibits convection into the outer convective envelope. However, by the time the star completes its evolution through the luminosity bump, the H-burning shell crosses the radiative zone barrier of mean molecular weight discontinuity and begins mixing processed material in the H-burning shell with the outer convective envelope (see Palacios et al. 2001; Denissenkov & Herwig 2004; Eggleton et al. 2008; Denissenkov & Merryfield 2011). Theoretical studies predict a further decrease in ^{12}C/^{13}C from the values of 20 to 30 post-first dredge-up, a decrease in ^{12}C, and enhancement in N abundance. The extra mixing process seems to continue as the star ascends the RGB, as evidenced by observations of very low values of ^{12}C/^{13}C (e.g., Gilroy 1989). If some kind of extra mixing is responsible for the very low values of ^{12}C/^{13}C, it is likely that the same process may be responsible for high Li abundances in some of the RGB stars, as many of the super Li-rich stars are also found to have very low values of ^{12}C/^{13}C (Kumar & Reddy 2009; Kumar et al. 2011). To meet the observed levels of Li abundances in super Li-rich giants, there must be an efficient mechanism by which ^7Be is produced in hotter layers ($\geqslant 10^8$ K) with seed nuclei of ^{3}He that is transported to cooler regions where ^7Be is converted to ^7Li (Cameron & Fowler 1971). To avoid the destruction of freshly produced Li, this has to be quickly transported to the outer layers. Given the internal changes to the stellar structure, the associated extra mixing at the bump (e.g., Palacios et al. 2001), and the positional coincidence of observed Li-rich K giants with the bump region in the HR diagram, many studies (Charbonnel & Balachandran 2000; Kumar et al. 2011) suggested that the luminosity bump may be the probable site for Li enhancement, unless their evolutionary status is misrepresented. There is no convincing data available that can rule out the possibility of the luminosity bump as the site for Li enhancement.

However, in the case of these two stars, it is quite unlikely that the bump is the site that explains the observed Li enhancement. This is because the timescale for low-mass stars to evolve from the bump to the RGB tip is about $\sim 10^8$ years (see Table 5 of Bharat Kumar et al. 2015 and references therein), which is very high compared to the Li depletion timescales that are in the order of $\sim 10^6$ years (Palacios et al. 2001). Thus, the enhanced Li abundance at the bump may not survive a star's evolution through the RGB tip. Also, the rarity of Li-rich giants suggests that Li enhancement is a transient phenomenon attributed to short Li depletion timescales.

Though few studies do report Li-rich stars beyond the luminosity bump and closer to the tip, their rate of occurrence seems to be much lower when compared to Li-rich stars at the bump and/or clump luminosities. To explain Li-rich stars in the narrow range of luminosity overlapping with the bump and the RC regions in the HR diagram as reported in Kumar et al. (2011), Denissenkov (2012) introduced rapid internal rotation for extra mixing at the bump, predicting giants making a zig-zag motion in the $T_{\rm eff}$-luminosity space in the HR diagram. However, the zig-zag motion theory cannot be applied as the two stars reported here are known to be at RC with core He-burning.

An alternative scenario is the Li enhancement at the RGB tip during the He-flash as suggested by Kumar et al. (2011). He-flash is associated with internal changes as the result of He-core ignition and deep convection. The multi-dimensional hydro-dynamic simulations in low-mass Population I models (Eggleton et al. 2008; Mocák et al. 2011) do predict H injection into He-burning shell convection at the core. This would further increase in ^{13}C (and hence low ^{12}C/^{13}C, below 10), ^{14}N, and also high Li, assuming that there is an ample amount of ^{3}He that survived from the previous evolution. Models also predict some increase in fresh ^{12}C, a byproduct of a *triple*-α reaction, depending on the star's metallicity and initial mass. Post He-flash, giants settle down at the RC region with a double-shell structure of He- and H-shell burning. Evolution from the tip to the RC region is quite fast, and one would expect the survival of Li for the short duration. The stars' large Li abundances and positions at the beginning of the Horizontal Branch (HB) in the HR diagram (See Figure 3) indicate that Li enhancement might have been a recent episode. Because He-flash at the RGB tip is an immediately preceding evolutionary event on the RGB, it will not be unreasonable to associate it with the large Li enhancement seen in these two RC stars. However, one cannot rule out the possibility of some kind of a recent merger of sub-stellar components or white dwarfs at the tip of the RGB.

Recent reports of more Li-rich giants and their locations all along the RGB in the HR diagram complicates the problem. In some cases, super Li-enhancement as high as A(Li) ~ 4.5 dex, have been reported in sub-giants and below the bump (Martell & Shetrone 2013; Casey et al. 2016; Li et al. 2018). Model predictions range from the diffusion of Li in a narrow range of $T_{\rm eff}$ (e.g., Deliyannis et al. 2002) and the large close-in giant planets' engulfment with material of unburnt Li (e.g., Aguilera-Gómez et al. 2016). It seems unlikely that any one of the proposed scenarios in the literature would explain all of the characteristics of Li-rich stars: very high Li, IR excess, very low ^{12}C/^{13}C ratios, rotation, and evolutionary status. For example, the engulfment of planets may happen anywhere along the RGB but it is more likely to be found for Li-rich K giants at either the bump or clump as giants spend more time at these phases. However, the engulfment proposal requires the injection of huge planetary mass material with unburnt Li to account for super Li-rich abundances such as in this study. Given the large convective masses of RGB stars, a recent study by Aguilera-Gómez et al. (2016) puts an upper limit of A(Li) ~ 2.2 dex through engulfment. Note that the limit does not include any extra (induced) mixing. Another important suggestion that has not been rigorously explored is that of Zhang & Jeffery (2013), who predicted the composition of early-type R and J stars (early AGB stars). The simulations of merger scenarios of He white dwarf of different masses with the He-core of RGB stars do predict the convection of processed material from He- and H-burning shells that include

higher ^{13}C, ^{14}N, and hence lower ^{12}C/^{13}C. Also, by inserting a small fraction of ^{3}He left over from the previous evolution in the RGB envelopes into the He-burning shell, they suggested that Li could be produced in the inner layers. However, all of the scenarios yield a post-merger final mass of $2\,M_\odot$, which is twice that of the stars in this Letter. Also the models predict IR excess as a result of the merger. Neither of the two stars show evidence of IR excess.

5. Conclusion

Though it is premature to rule out the luminosity bump as the Li-enrichment site, it is very unlikely that the current high level of Li abundances seen in these stars survived through post-bump evolution due to significantly large evolutionary timescales compared to Li depletion. The very high Li abundances and their position at the beginning of the HB suggest that Li enhancement, at least in these two candidates, occurred at the tip of the RGB, probably during He-flash. However, our current understanding of nucleosynthesis and the mixing process during He-flash is lacking and needs to be probed further. Also, it is not inconceivable that many Li-rich giants are in fact misclassified (see e.g., da Silva et al. 2006) and that they are most likely core He-burning stars. This argument may be strengthened by the fact that low-mass stars spend much longer time at RC, and as a result they have a higher probability of being detected as Li-rich stars. It is worthwhile to explore mechanisms such as the merger of a He white dwarf with a RGB star. These mergers may happen anywhere along the RGB, but post-merger stars can have He-burning cores.

ORCID iDs

Yerra Bharat Kumar ● https://orcid.org/0000-0003-2551-8124
Gang Zhao ● https://orcid.org/0000-0002-8980-945X

References

Aguilera-Gómez, C., Chanamé, J., Pinsonneault, M. H., & Carlberg, J. K. 2016, ApJ, 829, 127
Albareti, F. D., Allende Prieto, C., Almeida, A., et al. 2017, ApJS, 233, 25
Bharat Kumar, Y., Reddy, B. E., Muthumariappan, C., & Zhao, G. 2015, A&A, 577, A10
Brown, J. A., Sneden, C., Lambert, D. L., & Dutchover, E. J. 1989, ApJS, 71, 293
Cameron, A. G. W., & Fowler, W. A. 1971, ApJ, 164, 111
Casey, A. R., Ruchti, G., Masseron, T., et al. 2016, MNRAS, 461, 3336
Castelli, F., & Kurucz, R. L. 2004, arXiv:astro-ph/0405087
Charbonnel, C., & Balachandran, S. C. 2000, A&A, 359, 563
Cutri, R. M., et al. 2013, yCat, 2328, 0
Cutri, R. M., Skrutskie, M. F., van Dyk, S., et al. 2003, The IRSA 2MASS All Sky Point Source Catalog, NASA/IPAC Infrared Science Archive, http://irsa.ipac.caltech.edu/applications/Gator/
da Silva, L., Girardi, L., Pasquini, L., et al. 2006, A&A, 458, 609
Deliyannis, C. P., Steinhauer, A., & Jeffries, R. D. 2002, ApJL, 577, L39
Denissenkov, P. A. 2012, ApJL, 753, L3
Denissenkov, P. A., & Herwig, F. 2004, ApJ, 612, 1081
Denissenkov, P. A., & Merryfield, W. J. 2011, ApJL, 727, L8
Eggleton, P. P., Dearborn, D. S. P., & Lattanzio, J. C. 2008, ApJ, 677, 581
Gilroy, K. K. 1989, ApJ, 347, 835
Girardi, L. 2016, ARA&A, 54, 95
González Hernández, J. I., & Bonifacio, P. 2009, A&A, 497, 497
Hobbs, L. M., Thorburn, J. A., & Rebull, L. M. 1999, ApJ, 523, 797
Iben, I. J. 1967, ApJ, 147, 650
Jofré, E., Petrucci, R., García, L., & Gómez, M. 2015, A&A, 584, L3
Kjeldsen, H., & Bedding, T. R. 1995, A&A, 293, 87
Kumar, Y. B., & Reddy, B. E. 2009, ApJL, 703, L46
Kumar, Y. B., Reddy, B. E., & Lambert, D. L. 2011, ApJL, 730, L12
Kumar, Y. B., Reddy, B. E., & Zhao, G. 2018, JApA, 39, 25
Lambert, D. L., & Reddy, B. E. 2004, MNRAS, 349, 757
Li, H., Aoki, W., Matsuno, T., et al. 2018, ApJL, 852, L31
Lind, K., Asplund, M., & Barklem, P. S. 2009, A&A, 503, 541
Martell, S. L., & Shetrone, M. D. 2013, MNRAS, 430, 611
Mocák, M., Siess, L., & Müller, E. 2011, A&A, 533, 53
Monaco, L., Villanova, S., Moni Bidin, C., et al. 2011, A&A, 529, A90
Mosser, B., Benomar, O., Belkacem, K., et al. 2014, A&A, 572, L5
Palacios, A., Charbonnel, C., & Forestini, M. 2001, A&A, 375, L9
Pinsonneault, M. H., Elsworth, Y., Epstein, C., et al. 2014, ApJS, 215, 19
Ramírez, I., & Allende Prieto, C. 2011, ApJ, 743, 135
Rebull, L. M., Carlberg, J. K., Gibbs, J. C., et al. 2015, AJ, 150, 123
Reddy, B. E., Lambert, D. L., Hrivnak, B. J., & Bakker, E. J. 2002, AJ, 123, 1993
Reddy, B. E., Tomkin, J., Lambert, D. L., & Allende Prieto, C. 2003, MNRAS, 340, 304
Siess, L., & Livio, M. 1999, MNRAS, 308, 1133
Silva Aguirre, V., Ruchti, G. R., Hekker, S., et al. 2014, ApJL, 784, L16
Sneden, C., Lucatello, S., Ram, R. S., Brooke, J. S. A., & Bernath, P. 2014, ApJS, 214, 26
Sneden, C. A. 1973, PhD thesis, Univ. Texas
Szigeti, L., Mészáros, S., Smith, V. V., et al. 2018, MNRAS, 474, 4810
Tajitsu, A., Sadakane, K., Naito, H., Arai, A., & Aoki, W. 2015, Natur, 518, 381
Vrard, M., Mosser, B., & Samadi, R. 2016, A&A, 588, A87
Wallerstein, G., & Sneden, C. 1982, ApJ, 255, 577
Zhang, X., & Jeffery, C. S. 2013, MNRAS, 430, 2113
Zhao, G., Chen, Y.-Q., Shi, J.-R., et al. 2006, ChJAA, 6, 265
Zhao, G., Zhao, Y.-H., Chu, Y.-Q., Jing, Y.-P., & Deng, L.-C. 2012, RAA, 12, 723